Title
AN INDIRECT MEASUREMENT OF THE n-n INTERACTION

Author
Phillips, Robert Hastings.

Publication Date
1952-06-01

UCRL- 1845

UNCLASSIFIED

UNIVERSITY OF CALIFORNIA - BERKELEY

RADIATION LABORATORY

DISCLAIMER

UCRL-1845
Unclassified-Physics Distribution

UNIVERSITY OF CALIFORNIA

Radiation Laboratory

Contract No. W-7405-eng-48

AN INDIRECT MEASUREMENT OF THE n-n INTERACTION

Robert Hastings Phillips

(Thesis)

June, 1952

Berkeley, California

TABLE OF CONTENTS

AN INDIRECT MEASUREMENT OF THE n-n INTERACTION

Robert Hastings Phillips

(Thesis)

ABSTRACT

The gamma ray spectrum from the process $\pi^- + D \rightarrow 2n + \gamma$ has been measured using an improved 117-channel pair spectrometer. The pions were produced in an internal target by 335 Mev protons of the 184-inch cyclotron. Watson and Stuart have shown that the spectrum is sensitive to the n-n interaction and have calculated theoretical spectra based on the parameter α, the inverse "scattering length" which relates the results to the low energy n-n scattering cross section. The experimental data are analyzed by evaluating a weighted first moment of the spectrum. Comparison with weighted first moments of the theoretical spectra leads to a value of $\alpha^{-1} = -15.7 \times 10^{-13}$ cm with limits, based on the probable error, of $\alpha^{-1} = -8.7 \times 10^{-13}$ cm and $\alpha^{-1} = -\infty$ cm. The value $\alpha^{-1} = -15.7 \times 10^{-13}$ cm corresponds to an unbound state ($\sim$260 Kev positive) for the hypothetical dineutron. Taking $r_0 = 2.65 \times 10^{-13}$ cm, the total cross section for n-n scattering evaluated at zero energy, is approximately 31 barns.

I. INTRODUCTION

Low energy proton-proton scattering experiments permit the evaluation of two parameters of the nucleon-nucleon interaction[1]. In particular the results show[2] that the lowest singlet state for two protons is unstable. Except for coulomb repulsion effects, arguments based on the charge independence of nuclear forces would therefore predict that the lowest singlet states of the n-p and n-n systems would not be stable either. In the case of the n-p system, scattering experiments again bear this out[2]. Serious experimental difficulties, however, have precluded the use of scattering experiments to study the n-n forces. The present experiment permits the evaluation of one parameter of the n-n interaction.

Several papers have been written discussing the existence of the dineutron[3,4,5] and considerable experimental work has been done in an effort to establish its actuality[6-11].

Kundu and Pool[4] bombarded Co^{59} and Rh^{103} with tritium. The observed half lives of the products established the fact that the reaction had proceeded by capture of two neutrons. They concluded that the mechanism involved was probably the Oppenheimer-Phillips[12] process with H^3 rather than a compound nucleus mechanism. Capture by the Oppenheimer-Phillips process would suggest that the two neutrons may be captured as a group. This would mean that a dineutron could have at least transient existence in the instant between the polarization of the tritium nucleus and the capture. The experiment has a rather remote bearing on the actual occurrence of an observable dineutron.

N. Feather[5] has established the upper limit of the binding energy of the dineutron to be 0.7 Mev based on the fact that He^6 is stable against heavy particle emission. By consideration of a group of known reactions for which the Q values have been experimentally established he is able to deduce:

$$He^6 \longrightarrow He^4 + 2n - 0.7 \text{ Mev}$$

Using this limit and the known binding energy of the deuteron he is able to estimate the limits on the lifetime of the dineutron as between 1 and 5 seconds assuming a superallowed β disintegration.

Acting on a suggestion by N. Feather[5] that the dineutron, if stable, might be emitted in the process of fission and if so could be detected by capture in Bi^{209}, Fenning and Holt[6] irradiated Bi^{209} in the Harwell pile. The thermal flux of neutrons was about 10^{12} neutrons per sq. cm per sec. Denoting the flux of dineutrons by ϕ and the capture cross section by σ, they reported that no activity ascribable to A_cC was observed and set $\phi\sigma < 1.5 \times 10^{-21}$ per sec.

Feather gave a preliminary report[7] on an experiment by Fenning in which he had irradiated He^4 in the Harwell pile and apparently observed the approximately one second activity from He^6 in the reaction $He^4 + n^2 \longrightarrow He^6 \longrightarrow \beta^-$. It was later concluded that the observed activity was a result of contamination of the He^4 and that $\phi\sigma < 10^{-18}$ per sec. where σ is now the capture cross section of helium for dineutrons.

The experiments so far described only yield evidence on the existence of the dineutron. Beyond the establishment of limits on the "binding energy" of this hypothetical particle, they give no detailed information on the n-n interaction.

Los Alamos Scientific Laboratory[9] has reported evidence for the production of dineutrons in the reaction $T^3 + T^3 \longrightarrow He^4 + n^2$. A. Hemmindinger[10] gives more detail on this experiment. The reaction may proceed in three alternative ways:

1. $T^3 + T^3 \longrightarrow He^4 + 2n$
2. $T^3 + T^3 \longrightarrow He^4 + n^2$
3. $T^3 + T^3 \longrightarrow He^5 + n$, $\quad He^5 \longrightarrow He^4 + n$

The first process will give a continuous distribution of alpha particle energies. The second process would give a peak of Alpha particle energies depending on the angle of observation. Hemmindinger says a detailed kinematic analysis of the kinematics of the third process shows that two or more peaks of alpha particle energies, associated with a given angle, would be expected. But if the He^5 nucleus is in its ground state as determined by n-He^4 scattering measurements[13] the number of peaks for the He^5 process would be limited to two and one of these peaks would be of too low energy to be observed by their apparatus. At all angles the peak resulting from process (2) would appear at a higher energy than any of the peaks from process (3). Since two peaks are observed, the high energy peak is attributed to the emission of dineutrons. Hemmindinger states that "The dineutron appears to be unbound by a few hundred Kev", although no detailed calculations, based on the absolute energy calibration from the D(T,n) He^4 reaction, are given. In any case it seems possible that the high energy peak attributed to dineutron emission might really be the peak from the $D(T,n)He^4$ resulting from deuterium contamination of the target or beam. In the case of the unbound ("virtual") state it would also be difficult to preclude the fact that the peak resulted from two neutrons emitted singly under the action of an attractive potential.

Another group at Chalk River[11] have also investigated the T-T reactions by measurement of the disintegration products. They observe no alpha particle group with an energy equal or greater than that corresponding to an alpha particle recoiling from an emitted dineutron of zero binding energy. This enables them to put a limit on the occurrence of a bound dineutron as less than one per cent of the disintegrations. They also place an upper limit of one per cent of the disintegrations as resulting from the existence of the dineutron in a virtual state of energy $\leq$ 0.6 Mev of lifetime $\leq 3 \times 10^{-21}$ sec. Deuterium contamination prevents them from making more detailed observations in the energy region corresponding to the unstable dineutron.

It should be noted that no simple theory can be used to derive information on the n-n forces from the T-T process because of the interaction of the two neutrons with the alpha particle. Recent experimental work with mesons has opened up a new approach to the problem. Panofsky, Aamodt, and Hadley[14] have established that the capture of negative pions in deuterium may lead to either of the following processes:

$$\pi^- + D \rightarrow 2n$$
$$\pi^- + D \rightarrow 2n + \gamma$$

Tamor and Marshak[15,16] and Bruekner, Serber, and Watson[17] have pointed out that the gamma ray spectrum from the radiative capture process is influenced by the n-n interaction. Since there is no nuclear interaction between the two neutrons and the gamma ray, this process permits a simpler theoretical analysis.

Watson and Stuart[18], assuming a singlet S-state for the final state of the two neutrons, have calculated the theoretical spectra based on the phase shift which is directly related to the low energy n-n scattering cross section through the equation $\sigma_{n-n} = \frac{4\pi}{k^2} \sin^2 \delta$ Schwinger[19] has shown δ may be related, through the equation $k \cot \delta \approx -\alpha + \frac{1}{2} r_o k^2$ to two parameters used to describe the low energy scattering: α, the "scattering length" and r_o, the "effective range". They state that the spectra are not very sensitive to the exact value of r_o and as a result they assign to it the value obtained from p-p scattering: $r_o = 2.65 \times 10^{-13}$ cm[20]. Thus α becomes the convenient parameter in this description of the n-n interaction.

Comparison of previous experimental results[21] using the basic method described in this paper leads to a nominal value for the lowest state of the n-n system of 1.2 Mev virtual, equivalent to a value of $\hbar c \alpha \approx 33$ Mev. The energy resolution of this experiment, however, was too poor to exclude either the bound or no-interaction case. It therefore seemed desirable to seek an improvement in the measurement with better resolving power. The present experiment was accordingly undertaken.

II. EXPERIMENTAL METHOD

A. Basic Method

The capture of negative pions[14] at rest in hydrogen yields a monoenergetic gamma ray since it is a two body process: $\pi^- + p \longrightarrow n + \gamma_H$. The capture of negative pions at rest in deuterium[14] yields a spectrum of gamma rays influenced by the n-n interaction: $\pi^- + D \longrightarrow 2n + \gamma_D$. The case where the two neutrons come off together, but without interaction determines the energetic upper limit for the unbound state. Conservation of energy and momentum gives

$$E_{\gamma_{D_{max}}} = \frac{(M_\pi + M_D)^2 - 4 M_n^2}{2(M_\pi + M_D)} \tag{1}$$

$$E_{\gamma_H} = \frac{(M_\pi + M_p)^2 - M_n^2}{2(M_\pi + M_p)} \tag{2}$$

Thus

$$E_{\gamma_{D_{max}}} - E_{\gamma_H} = M_D - (M_p + M_n) - \frac{1}{n}\left(\frac{E_{\gamma_{D_{max}}}^2}{4} - \frac{E_{\gamma_{D_{max}}}^4}{16 n^3} - \frac{E_{\gamma_H}^2}{2} + \frac{E_{\gamma_H}^4}{8 n^3} + \cdots\right) \tag{3}$$

$E_{\gamma_{D_{max}}} - E_{\gamma_H}$ determines the position of the theoretical spectra on the energy scale relative to E_{γ_H} and is not sensitive to the value assumed for E_{γ_H} (see Sec. II, D). The theoretical spectra, corrected for the resolution of the instrumentation, may thus be compared with the experimental data for $\pi^- + D \longrightarrow 2n + \gamma_D$ without exact evaluation of the absolute energy scale provided both capture processes are observed with identical instrumentation. A mere change of the gas used as the capturing substance made this possible in the present instance.

B. General Arrangement

Negative pions are produced by bombarding a heavy-element target with the internal proton beam of the 184-inch Berkeley synchrocyclotron. Some of the pions are then absorbed in deuterium in the form of a high pressure gas confined in a cylinder contiguous to the proton beam target. Some of the gamma rays emitted in the reaction $\pi^- + D \longrightarrow 2n + \gamma_D$ are permitted to enter a pair spectrometer through a collimating system (Fig. 1). Details of this experimental arrangement are completely explained in the paper by Panofsky et al[14].

The events comprising the data, "pairs", are coincidences between pair fragments (see Fig. 1) which are detected by both banks of geiger tubes. The geiger tubes are gated by "gated quads", a quadruple coincidence between both sides of both proportional counters in coincidence with a beam pulse gate. A measurement of the energy of the pair fragments determines the energy of the incident gamma ray.

The present pair spectrometer has been designed by K. Crowe to achieve greatly improved energy resolution by means of first order horizontal angular focusing and a decrease of the energy aperture of the pair-detecting geiger counters.

Figure 2 is a schematic drawing to show how first order horizontal angular focusing results from the geometry used. In practice the electrons pass through a fringing field which means that the determination of the actual focus line depends on careful measurement of the field in order to plot exact orbits.

An increased number of geiger tubes were arranged to overlap each other so that the energy defining aperture was reduced to 0.75 Mev (Fig. 3).

Since experimental results have been shown to be essentially independent of an absolute energy scale, a more detailed analysis of the pair spectrometer is unnecessary except insofar as the resolution or detection efficiency is energy dependent.

C. Operation of the Runs

The entire running time extended continuously over a period of ten days. The net data collection time was 37.8 hours for deuterium, 26.0 hours for hydrogen, and 22.1 hours for background. Plateaus for the proportional counters and associated electronics were established by the gamma ray flux from neutral pion decay[22] at the start of the experiment. This is a fairly time consuming procedure and was therefore only repeated once when required by replacement of one of the proportional counters. The geiger tubes and associated electronics were individually checked before the start of the experiment and at the end of each day by means of a radioactive source; they were also checked occasionally during the runs by ungating. No replacements were necessary. The magnetic field was maintained constant throughout the experiment by monitoring with a nuclear fluxmeter.

An attempt was made to monitor the proton beam intensity by means of a neutron counter mounted inside the shielding about four feet from the cyclotron tank and directly along the line of sight of the beam and the primary target. A buildup of the activity level on the platform over the daily 16-hour bombardment periods may to some extent invalidate this as an instantaneous indicator of beam intensity.

D. The Folding Procedure

The theoretical spectra, as mentioned in part A, must be corrected for the resolution of the instrumentation. The pair spectrometer because of its finite resolving power detects a distribution of energy values about E_{γ_H} instead of a monochromatic line from the process $\pi^- + p \longrightarrow n + \gamma_H$. The gamma ray spectrum from the capture in hydrogen, $I_{\gamma_H}(E)$ thus defines the resolution of the instrumentation. Provided this resolution curve is not energy dependent it may be folded into the various theoretical spectra for comparison with the experimental results.

The folding operation is $\phi(E) \equiv \int I(t)\, R\,(t-E)\, dt$ where $I(t)$ is the theoretical spectrum and $R(t)$ is the resolution curve (the kernel) which describes the observed distribution of energy values around the assigned value (the origin of $R(t)$). In general, the assigned value must be determined by a theoretical analysis of the characteristics of the instrumentation which produce the spread in the observed energy values. The evaluation of the present results, however, will be shown to be independent of the assigned value of the kernel to the first order. The higher order error introduced is much smaller than the probable error of the measurement.

The assigned value of the kernel here represents the measured value E_{γ_H} and is thus the origin in a plot of $R(t) \equiv I_{\gamma_H}\left[-(E - E_{\gamma_H})\right]$ where I_{γ_H} (shown in Figure 3 as fitted to the data) has been corrected for the known energy dependent efficiency of the pair spectrometer (See Part E, below). As shown in Part A the absolute energy scale of the theoretical spectrum, $I(t)$, is uniquely determined by this measured value of E_{γ_H} and the dynamics of the two capture processes. A change ($-\Delta E$) in the measured value of E_{γ_H} results in a change ($+\Delta t$) in the assigned value of the kernel such that the kernel now becomes $R(t+\Delta t)$. The units of E and t are equal here. But this change in E_{γ_H} also changes the upper limit (for the case of negative α values[18]) of I(t) by an amount that exactly compensates for the change in R(t). Thus the resulting fold, $\phi(E)$, is the same in both cases.

For an assigned value E_{γ_H} the fold is $\phi(E) = \int I(t) R(t-E)\, dt$

For an assigned value $E_{\gamma_H} + \Delta E$ the fold is: $\phi(E) = \int I(t+\Delta t)\, R[(t+\Delta t) - E]\, dt$

Since both I(t) and R(t) have been shifted by the same amount, Δt, the integrated product of the two functions is unchanged for any given value of E (Fig. 4).

Equation (3) on page 7 shows that $E_{\gamma_{D\max}} - E_{\gamma_H}$ is not sensitive to the absolute value of E_{γ_H}. Differentiating Equation (3) gives:

$$\frac{d\left(E_{\gamma_{D\max}} - E_{\gamma_H}\right)}{d E_{\gamma_H}} \approx \frac{E_{\gamma_H}}{n} - \frac{E_{\gamma_{D\max}}}{2n} \frac{d E_{\gamma_{D\max}}}{d E_{\gamma_H}} + \dots$$

Now one can easily show $\quad \dfrac{d E_{\gamma_{D\max}}}{d E_{\gamma_H}} \approx 1$

so

$$\frac{d\left(E_{\gamma_{D\max}} - E_{\gamma_H}\right)}{d E_{\gamma_H}} \leq \frac{1}{n}\left(E_{\gamma_H} - \frac{E_{\gamma_{D\max}}}{2}\right)$$

An exact calculation gives:

$$\Delta\left(E_{\gamma_{D\max}} - E_{\gamma_H}\right) = 0.06\, \Delta E_{\gamma_H} \text{ (Mev)}$$

for the error in the position of the theoretical spectra due to an error in the assigned value, $E\gamma_H$, of the kernel. Watson and Stuart[18] assumed a value of $E\gamma_{D_{max}} = 132.00$ Mev which corresponds to an assigned value $E\gamma_H = 129.72$ Mev. This value of $E\gamma_H$ is close to a preliminary estimate of the experimental value as measured by Crowe[23]. It seems doubtful that $\Delta E\gamma_H$ will turn out to be greater than one Mev. This would mean a correction of 0.06 Mev, roughly a factor of ten smaller than the probable error assigned to the final measurement. In any case the above formula gives a simple method of adjusting the final results. The folded theoretical spectra are shown in Fig. 5.

E. Energy Dependent Factors

It is important that no energy dependent losses distort the observed gamma ray spectra. Multiple scattering in the converter is a source of energy dependent losses in the observed intensity of gamma rays. The defocusing effect of the fringing field is not independent of the energy of the vertically scattered electrons. As a result they are scattered into a solid angle which is energy dependent whereas the vertical defining aperture of the geiger tubes is constant. The rather large (three square inches) converter used will magnify this effect. Fortunately, there is a good experimental check on this point. During the course of the associated study of the pion capture in hydrogen[23] it was necessary to evaluate the yield of pairs as a function of converter thickness. This was done by directly observing the gamma rays from the decay of neutral pions[22] produced by the proton bombardment of the primary target. These results are plotted in Fig. 6 together with some recent results of Crandall[24] using a one-inch square converter. Crandall has done a careful analysis of energy dependent losses and his curve has been corrected for these effects. His primary target was carbon, but it has been shown[25] that the spectra for carbon and heavy elements are indistinguishable. It is seen that no significant losses occur except at the ends of the spectrum which are far from the region of interest for both capture processes as will become apparent later in this section.

A known source of energy dependence of the detection efficiency of the pair spectrometer results from its finite size since it detects a variable fraction of the possible pair combinations for a given E_γ. A correction for this effect is easily calculated from the known geometry of the geiger counter[24,26] array.

The correction for the variation of the pair production cross section as a function of energy was taken from Heitler[27]. The maximum effect was less than $1\frac{1}{2}$ per cent for $I(\gamma_D)$. No correction is necessary for $I(\gamma_H)$ since E_{γ_H} is monochromatic.

$R(t) \equiv I_{\gamma_H}\left[-(E-E_{\gamma_H})\right]$, as pointed out, must not be energy dependent. The final analysis of the data (see Part G, below) is based on evaluation of the first moment of the folded theoretical curves. The fold with $R(t-E)$ will only result in an error in the evaluation of the first moment of the folded theoretical curves if the first moment of $R(t)$ is energy dependent. A preliminary theoretical analysis of the resolution curve of the pair spectrometer has been made by K. Crowe[23] involving consideration of energy channel width, converter size, radiation straggling of the pair in the converter, energy loss resulting from ionization by the pair and multiple scattering of the pair in the converter. Only energy loss from ionization and radiation straggling will produce asymmetry in the resolution curve and hence result in an energy dependent shift of its first moment. Crowe[23] finds the probability of the energy loss from ionization is constant up to a cut-off value of 1.4 Mev for the converter used. Using this cut-off value a calculation based on the dE/dx curves given by Halpern and Hall[28] shows that the shift from this source is less than 10 Kev from 120 to 135 Mev, the range of the fold. This effect is thus negligible.

The probability, $W(y)dy$, that an electron will retain e^{-y} times its initial energy in traversing a thickness of the converter is given by Heitler[29]. By a change of variable the probability, $W(\frac{E}{E_o})dE$, that the electron retains a fraction $\frac{E}{E_o}$ of its initial energy E_o (Fig. 7) is:

$$W\left(\frac{E}{E_o}\right)dE = \frac{\Gamma(bl)}{E_o\left(\log\frac{E_o}{E}\right)^{1-bl}}\,dE \qquad bl \leq 0.1$$

The calculation of the first moment of $W(\frac{E}{E_o})$ shows that the shift is less than 30 Kev in the range of the fold and is therefore of no importance.

The first order calculation[23] of the theoretical resolution curve checks well with the experimental γ_H spectrum. However, the theory does show that a low energy tail to the γ_H signal would be expected. Experimentally, as mentioned in Part G below, the tail is at the high energy end of the spectrum as can be seen by inspection of Fig. 3. But the intensity of the tail is so low that it has no influence on the final result. This small effect may be due to a time variation in the sensitivity of the proportional counters. The geometry is such that high energy pairs have a longer path length in the proportional counters and therefore a greater probability of being recorded at lower efficiency.

There was in fact some indication of a slight deterioration of the sensitivity of the proportional counters during the run.

R(t) must of course be corrected for the variation in the sensitivity of the pair spectrometer resulting from the fact that it detects a variable fraction of the possible combinations of pair fragments for a given E_γ as mentioned previously.

Uncertainty in the theoretical curves in the energy region below 120 Mev will result in an insignificant error in the final folded theoretical curves because both the theoretical curves and the kernel have low values in this region. The effect was checked by a fold performed omitting the tail below 120 Mev of the theoretical spectrum for $\hbar c \alpha = -\infty$. This spectrum was chosen because it would show the maximum effect since it has the largest values below 120 Mev of any of the theoretical spectra. The result is shown in Fig. 8. A calculation based on the analysis of the data as described in Part G below shows that this procedure results in less than a three per cent error in evaluating the spectrum for $\hbar c \alpha = -\infty$ for comparison with the experimental results. Since the theoretical data below 120 Mev are certainly valid to some extent the effect on the fold of any error in this region is insignificant.

F. Background Factors

Consideration must be given to the fact that processes other than the radiative capture of the negative pion may have taken place when the deuterium was introduced. Besides negative pions, positive and neutral pions, protons, neutrons, and gamma rays are produced by the 340 Mev protons incident on the heavy element primary target. Some of these particles can certainly give rise to high energy gamma rays when they interact with the deuterium. These interactions are now listed in order of their importance.

1. Charge exchange scattering of either positive or negative pions can produce neutral pions with their consequent high energy decay gammas. A calculation based on the charge exchange cross section for negative pions reported by Fermi et al[30] and assuming charge symmetry[31] gives an effect which is less than one per cent of the measured radiative capture. Wilson and Perry[32] observed a cross section for charge exchange scattering of positive pions in deuterium which confirms this limit.

Strong evidence that charge exchange scattering is negligible in the present experiment is given by the result of previous experimental work on the capture of negative pions in deuterium[14,26]. Attempts to observe gamma emission from neutral pions resulted in a null effect.

2. Direct production of neutral pions by stray high energy particles incident on the deuterium would also have shown up in the previous deuterium capture experiments. The null effect mentioned above rules this out.

3. The cross section for in-flight radiative capture of pions in hydrogen calculated by detailed balancing, gives a result less than one per cent of the charge exchange cross section. This source of high energy gammas is thus altoghether negligible.

The accidental ungated quad rate was approximately 1.3 counts per minute compared with a total gated quad rate of 2.6 counts per minute. The data, however, show very little evidence of accidental influence. Triples (coincidences between three geiger channels), double pair and other peculiar events comprise less than ten per cent of the data whereas the "singles", gated geiger counts of only one pair fragment, give approximately the same counting rate as the pairs.

G. Treatment of the Data

The reduction of the raw data from the pion capture reactions requires the normalization of the background counts to those of the γ_H and γ_D signal. The background runs are made by evacuating the high pressure gas cylinder. Any normalization procedure depends on some method of evaluating the relative beam intensity and detection efficiency from one type of run to another. So much beam time would have been lost to pumping procedure that no attempt was made to alternate short runs of deuterium, hydrogen, and background.

To explain attempted normalization procedures the following notation is used. "Doubles" are coincidences between both sides of a single proportional counter. "Ashbys" are neutron monitor counts. "Gated quads" and "pairs" were defined in Part B.

"Doubles" were investigated as a method of monitoring. Comparison of various ratios however such as "doubles"$_1$/"doubles"$_2$, "pairs"/"doubles", and "gated quads"/"doubles" does not show an internal consistency for runs of a given type (i.e., hydrogen gas, deuterium gas, or vacuum) which is reliable to ten per cent. In addition "doubles" would be sensitive to any change in the detection efficiency of the proportional counters. Ratios of "doubles"/"Ashbys", "gated quads"/"Ashbys", "pairs"/"Ashbys" also show erratic fluctuations.

The following normalization procedure was the one finally adopted. The magnitude of the probable errors of the data were not small enough to warrant analytical curve fitting. The background data were therefore averaged over three energy channels using a simple arithmetical mean. A smooth curve was drawn through the result. The curve was adjusted to the data by a careful attempt to balance probable errors. This process was repeated independently for the two other possible ways of combining the results of three energy channels. The values of all three smoothed curves were tabulated at one Mev intervals and averaged to give the values for the final smoothed background curve, which was plotted on semilog paper. This same procedure was carried out for the γ_H and γ_D signal data. A small correction was made to the γ_D spectrum for contamination of the deuterium by hydrogen. A mass spectrograph analysis of the deuterium showed a maximum of 1.25 per cent and a minimum of 0.25 per cent, depending on an unknown fraction of D^+ from fragmentation of HD[33]. The effect is so small that the extra effort to obtain an exact result was not considered worthwhile and an average value of 0.75 per cent was used for the correction factor.

The preliminary theoretical resolution curve[23] mentioned above shows that the half-width of the γ_H signal cannot exceed three Mev and the signal must be below one per cent of its peak value beyond ten Mev on either side of the peak. It is, therefore, possible to normalize the background to the γ_H signal by matching slopes of the two curves excluding the region within ten Mev of the peak of the γ_H signal (Fig. 9). It is estimated that this normalization is good to better than five per cent. In any case, because of the strong peaking of the signal as a result of the improved resolution, the resulting folded theoretical spectra are quite insensitive to a five per cent change in the normalization factor. This was checked by comparing resolution curves resulting from two different normalization factors. The two curves were indistinguishable well within the probable errors.

It will be noticed that the background data fits too high in the low energy portions of the curves and is balanced by too low a fit in the high energy portion. Adjusting the fit (five per cent lower) so that the background agrees best throughout the low energy portion simply adds a long, very low intensity tail to the resolution curve (approximately one count per channel). If the fit were adjusted seven per cent higher it would be in best agreement with the high energy portion which, however, includes less statistics than the low energy portion.

The normalization of the γ_D signal is not so straightforward. Here no assumption may be made regarding the limitation of signal intensity in the energy region below the peak since the shape of the spectrum is unknown. The background was therefore normalized using three different factors: 1. best fit; 2. fit to high energy signal; and 3. fit to low energy signal (Fig. 10). The final result was evaluated using all three factors to check the sensitivity of the data to the background normalization. The high and low normalization gives a result in disagreement at most 0.28 Mev. This effect is included in the probable error. It will be noted that the region of energy dependent losses as shown in Fig. 6 lies beyond any significant γ_D signal for any of the three normalization factors.

In Fig. 11 are shown the raw data which comprise the background, the γ_H signal, and the γ_D signal. The smoothed background curve as finally normalized is also shown. After the background normalization factors were established the smoothed background was subtracted from the raw γ_H and γ_D signal data. The result (Fig. 12) was corrected for energy dependent factors (Part E).

The analysis of the data was made by evaluating a weighted first moment of this net experimental data for comparison with the weighted first moment of the folded theoretical curves. The weighted first moment, M, was determined as follows:

$$M = \frac{\sum \frac{N_i F_i}{W_i^2} x_i}{\sum \frac{N_i F_i}{W_i^2}}$$

where $$W_i^2 = \frac{\left[0.675 \sqrt{\frac{m_{i-1} + m_i + m_{i-1}}{3}}\, \mathcal{N} \right]^2 + (0.675)^2 n_i}{N_i^2}$$

m_i ≡ number of counts in channel i of the background effects

n_i ≡ number of counts in channel i of the γ_D spectrum

N_i ≡ $n_i - m_i$

F_i ≡ energy dependent correction factor (Sec. II, D)

$\mathcal{N}$ ≡ background normalization factor.

The same weights, W_i, were used in the determination of the weighted moment of the experimental data and the theoretical curves. The probable error of the calculated value of M was determined by the law of propagation of errors.

Since $$M = \frac{\sum f(N_i)}{\sum g(N_i)}$$

then $$\delta M_j = \frac{\left[\sum g(N_i)\right]\frac{\partial f}{\partial N_j} - \left[\sum f(N_i)\right]\frac{\partial g}{\partial N_j}}{\left[\sum g(N_i)\right]^2}\,\delta N_j$$

and $$\delta M = \sqrt{\sum (\delta M_j)^2}$$

M was considered as a function of one variable only, N_i. The contribution to the error in M from the error in the combined probable error of the signal and background is of the second order and was neglected.

M was determined for all three background normalization factors for the γ_1 spectrum. The quoted value of M is based on the "best fit" (see above). The two other normalization factors resulted in M values differing by $\Delta M = +0.18$ Mev (using background fit to high energy signal) and $\Delta M = -0.13$ Mev (using background fit to low energy signal). The final error was evaluated as:

$$\sqrt{(\delta M)^2 + (\Delta M)^2}$$

III. RESULTS AND CONCLUSIONS

The parameter chosen for comparison of the experimental data with the theory is the weighted first moment as defined above. The position of Watson and Stuart's theoretical spectra[18] on the energy scale, relative to the observed γ_D spectrum, is established by the observed γ_H spectrum as described under the folding procedure. The most probable value of $\hbar c \alpha$ corresponding to the observed γ_D spectrum is then determined in the following manner. The weighted first moments of all the theoretical curves are plotted in Fig. 13 relative to that of the spectrum for $\hbar c \alpha = 0$ Mev as a function of $\hbar c \alpha$. A smooth curve is drawn through these points. The weighted first moment of the experimental γ_D spectrum relative to that of the spectrum for $\hbar c \alpha = 0$ Mev is -0.43 Mev with a probable error of $^{+0.43}_{-0.40}$ Mev. This value is plotted on the curve and the corresponding value of $\hbar c \alpha$ may be determined by inspection. This leads to an $\hbar c \alpha = -12.6 ^{+12.6}_{-10.2}$ Mev or $\alpha^{-1} = -15.7 \times 10^{-13}$ cm with limits, based on the probable error, of $\alpha^{-1} = -8.7 \times 10^{-13}$ cm and $\alpha^{-1} = \infty$, the limiting value separating unbound and bound states.

It is seen that the results essentially rule out the "no interaction" case ($\hbar c \alpha = -\infty$) which lies outside the measured value by 6 probable errors. The probable error is still too large, however, to conclude that the dineutron is definitely unbound.

An approximate evaluation of the cross section for low energy neutron-neutron scattering may now be made. Using the Equations on page 7 it may easily by shown:

$$\sigma_{n-n} \approx \frac{4\pi}{\alpha^2 + k^2 - r_0 k^2 \alpha + \frac{r_0^2 k^4}{4}}$$

The total cross section for low energy n-n scattering has been calculated based on the value of $\alpha^{-1} = -15.7 \times 10^{-13}$ cm as deduced above and $r_o = 2.65 \times 10^{-13}$ cm from p-p scattering[20]. The result is shown in Fig. 14. σ_{n-n} for E = 0 is 30.8 barns.

IV. ACKNOWLEDGMENTS

I am indebted to Dr. W. K. H. Panofsky for his inspiration and patient assistance throughout this work. The basic experimental arrangement was conceived by him for the pioneer negative pion capture experiments. Dr. Herbert York has offered many valuable suggestions and has kindly discussed many of the problems which arose in the analysis of the data. Mr. Kenneth Crowe is responsible for the design of the improved pair spectrometer. He has also done a detailed analysis of the spectrometer resolving power. His participation during the actual course of the experiment and in many discussions regarding the experimental procedure and the interpretation of the data was indispensible. Drs. Watson and Stuart kindly made available their original data for the "folding" process. Much valuable information was gained from discussions with Dr. Warren Heckrotte and Dr. Louis Henrich. Mrs. Ardith Kenney graciously devoted many hours of her spare time to the tedious calculations. Dr. Amos Newton performed the mass spectrograph analysis of the deuterium. Mr. John Harvie, Mr. Lu Whitcomb, Mr. L. R. Elliot, Mr. Leo Lambert, and Mr. John Kohot and Mr. Manuel Alcalde have been unusually patient with what must have seemed unreasonable demands on the machine shop. In addition, they were all of special aid in the detailed design of the equipment. The complicated electronics was maintained in excellent condition by Mr. Robert Barrere and Mr. Alexander Stripeika. The cyclotron crew under Mr. James Vale and Mr. Lloyd Hauser were especially cooperative in the after-hour "tank" sessions. The complexity of the experiment required much help during the collection of the data and the assistance of the many who are not specifically mentioned above is gratefully acknowledged.

Finally, I wish to express my deep gratitude for the constant encouragement from my wife, Betty Phillips.

V. REFERENCES

1. J. M. Blatt and J. D. Jackson, Phys Rev 76, 18 (1949)
2. H. A. Bethe and R. F. Bacher, Rev Mod Phys, 8, 133 (1936)
3. M. Y. Colby and R. N. Little, Jr., Phys Rev 70, 437 (1946)
4. D. N. Kundu and M. L. Pool, Phys Rev 73, 22 (1948), Phys Rev 82, 305A (1951)
5. N. Feather, Nature 162, 213 (1948)
6. F. W. Fenning and F. R. Holt, Nature, 165, 722 (1950)
7. N. Feather, Report of an International Conference on Elementary Particles, Tata Institute of Fundamental Research (December, 1950), printed by the Commercial Printing Press, 34-38 Bank Street, Fort, Bombay, India.
8. Private communication from F. W. Fennings to W. K. H. Panofsky
9. Los Alamos Scientific Laboratory, Phys Rev 79, 238A (1950)
10. A. Hemmendinger, TID-372, Oak Ridge (1950)
11. K. W. Allen, E. Almquist, J. T. Dewan, T. P. Pepper, and J. H. Sanders, Phys Rev, 82, 262 (1951)
12. J. R. Oppenheimer and M. Phillips, Phys Rev, 48, 500 (1935)
13. S. Bashkin, B. Petree, F. P. Mooring, and R. E. Peterson, Phys Rev, 77, 748A (1950)
14. W. Panofsky, R. Aamodt, and J. Hadley Phys Rev 81, 565 (1951)
15. S. Tamor and R. Marshak, Phys Rev 80, 766 (1950)
16. S. Tamor, Thesis, University of Rochester, 1950
17. K. Brueckner, R. Serber, and K. Watson, Phys Rev 81, 575 (1951)
18. K. Watson and R. Stuart, Phys Rev 82, 738 (1951)
19. J. Schwinger, Phys Rev 72, 742A (1947); hectographed notes on nuclear physics, Harvard, 1947
20. J. D. Jackson and J. M. Blatt, Rev Mod Phys, 22, 77 (1950)

21. R. Aamodt, W. Panofsky, R. Phillips, Phys Rev 83, 1057 (1952)

22. R. Bjorklund, W. Crandall, B. Moyer and H. York, Phys Rev 77, 213 (1950)

23. K. Crowe, private communication

24. W. E. Crandall, Thesis, University of California, 1952

25. K. M. Crowe, W. K. H. Panofsky, R. H. Phillips, and D. Walker, UCRL-1270 (Abstract); Phys Rev 83, 893A (1951)

26. R. L. Aamodt, Thesis, University of California, 1951

27. W. Heitler, The Quantum Theory of Radiation, Oxford University Press, 2nd ed., p. 201

28. O. Halpern and H. Hall, Phys Rev 73, 484 (1948)

29. W. Heitler, loc. cit. p. 225

30. E. Fermi, H. L. Anderson, A. Lundby, D. E. Nagle, and G. B. Yodh, Phys Rev 85, 935 (1952)

31. K. A. Brueckner, Phys Rev 86, 106 (1951)

32. R. Wilson and J. P. Perry, Phys Rev 84, 163 (1951)

33. R. A. Friedel and A. G. Sharkey, Jr. Chem Phys 17, 584 (1940)

VI. FIGURE CAPTIONS

1. Schematic of geometrical arrangement of apparatus.

2. Schematic diagram to show how first order horizontal angular focusing of the pairs is achieved. The geiger tube array is grouped about the focus line as shown in the insert.

3. $I_{\gamma_H}(E)$, the energy spectrum of the gamma ray from the process: $\pi^- + p \longrightarrow n + \gamma_H$ with background subtracted. The data have been corrected for energy dependent factors (Sec. II, E).

4. Schematic plots to show that the fold $\varphi(E)$ is unaffected by a change $(+\Delta t)$ in the assigned value of the kernel. The solid vertical line designates the assigned value of the kernel in each case.

5. Plot of the folded theoretical spectra; i.e., the theoretical spectra as deduced by Watson and Stuart[18] folded with the resolution function, $R(t - E)$.

6. Comparison of the gamma ray spectrum from π^0 production, measured by present pair spectrometer, with a spectrum due to Crandall[24] corrected for energy dependent losses.

7. Expected distribution of measured energy values because of radiation straggling by the pair in the converter. A primary energy, $E_0 = 65$ Mev, has been assumed for the electron.

8. Fold of the kernel with the theoretical spectrum for $\gamma_{c\alpha} = -\infty$ showing result of omitting the tail below 120 Mev of the theoretical spectrum.

9. Smoothed gamma ray spectrum from $\pi^- + p \longrightarrow n + \gamma_H$ showing normalization of smoothed background spectrum. Both curves are uncorrected for energy dependent factors (Sec. II, E). The peak structure is omitted.

10. Smoothed gamma ray spectrum from $\pi^- + D \longrightarrow 2n + \gamma_D$ showing all three normalizations of smoothed background spectrum. Both curves are uncorrected for energy dependent factors (Sec. II, E).

11. Unadjusted data showing gamma ray spectra from (1) $\pi^- + p \longrightarrow n + \gamma_H$; (2) $\pi^- + D \longrightarrow 2n + \gamma_D$; (3) background effects. All data are uncorrected for energy dependent factors (Sec. II, E). The best fit of the smoothed background spectrum is shown in each case.

12. Gamma ray spectrum from $\pi^- + D \rightarrow 2n + \gamma_D$ with background subtracted. The data have been corrected for energy dependent factors (Sec. II, E). Both linear and semi-log plots are shown with the statistical probable error.

13. Plot of the shift of the weighted first moment of the theoretical gamma ray spectra from $\pi^- + D \rightarrow 2n + \gamma_D$ relative to the theoretical spectrum for $\hbar c\alpha = 0$ Mev. The position of the weighted first moment of the experimental data relative to the theoretical spectrum for $\hbar c\alpha = 0$ Mev is shown with the calculated probable error.

14. Total cross section for low energy n-n scattering based on the value of the scattering length $\alpha^{-1} = 15.7\times10^{-13}$ cm as determined in Sec. III.

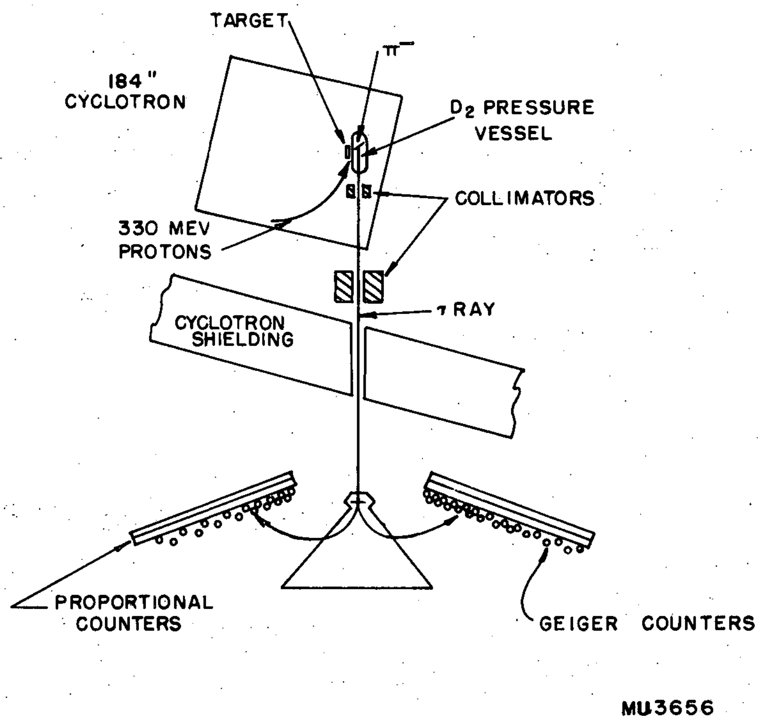
TARGET
π^-
184"
CYCLOTRON
D_2 PRESSURE
VESSEL
COLLIMATORS
330 MEV
PROTONS
γ RAY
CYCLOTRON
SHIELDING
PROPORTIONAL
COUNTERS
GEIGER COUNTERS
MU3656

Fig. 1

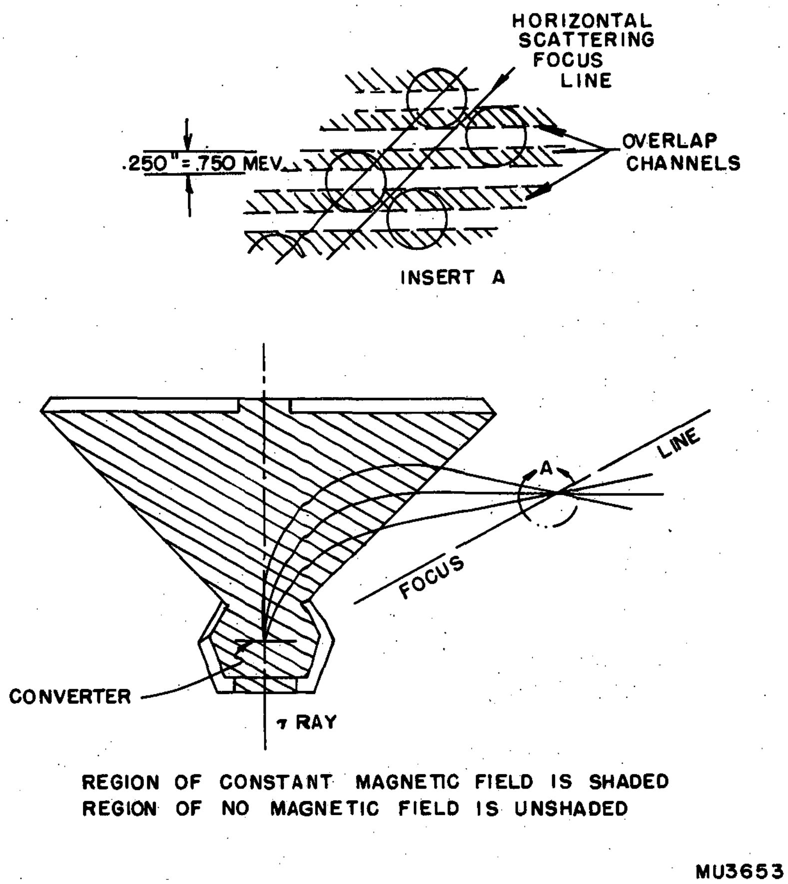
HORIZONTAL
SCATTERING
FOCUS
LINE
OVERLAP
CHANNELS
.250" = .750 MEV
INSERT A
LINE
A
FOCUS
CONVERTER
γ RAY
REGION OF CONSTANT MAGNETIC FIELD IS SHADED
REGION OF NO MAGNETIC FIELD IS UNSHADED
MU3653

Fig. 2

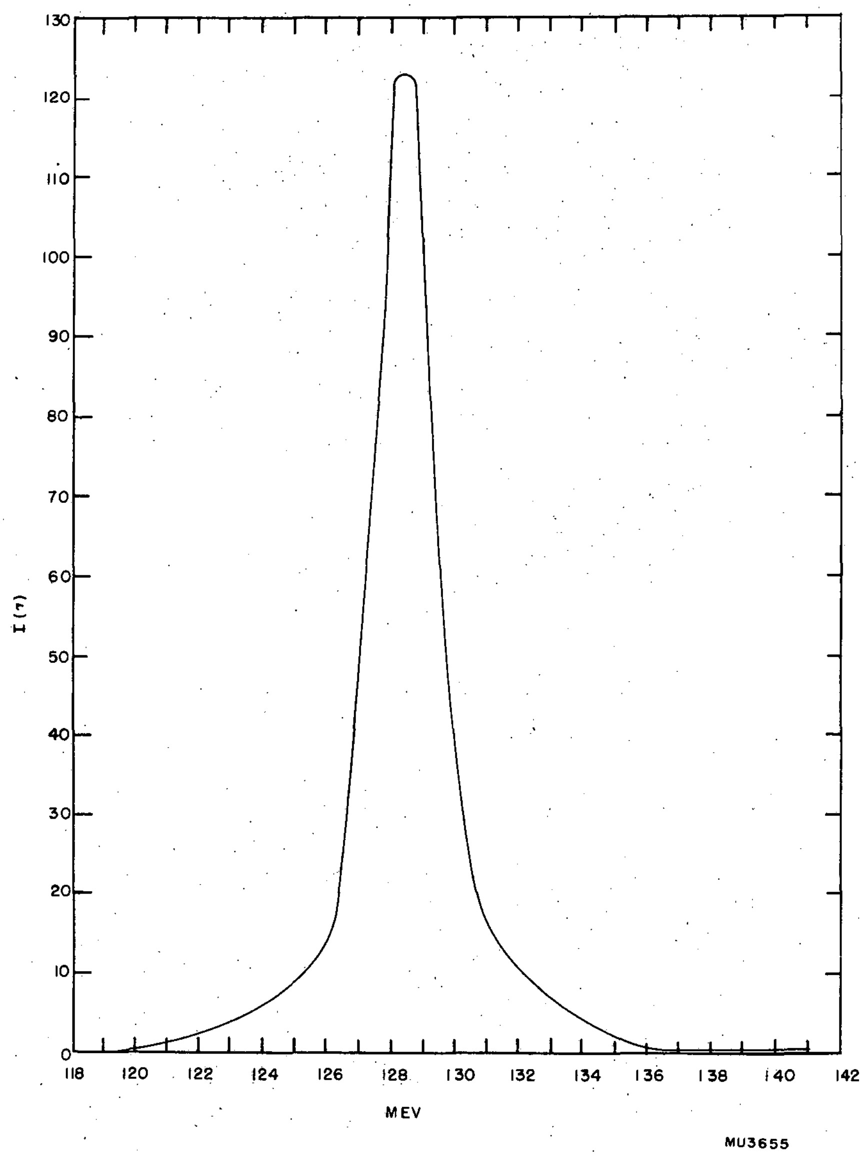
130
120
110
100
90
80
70
60
50
40
30
20
10
0
I (γ)
118
120
122
124
126
128
130
132
134
136
138
140
142
MEV
MU3655

Fig. 3

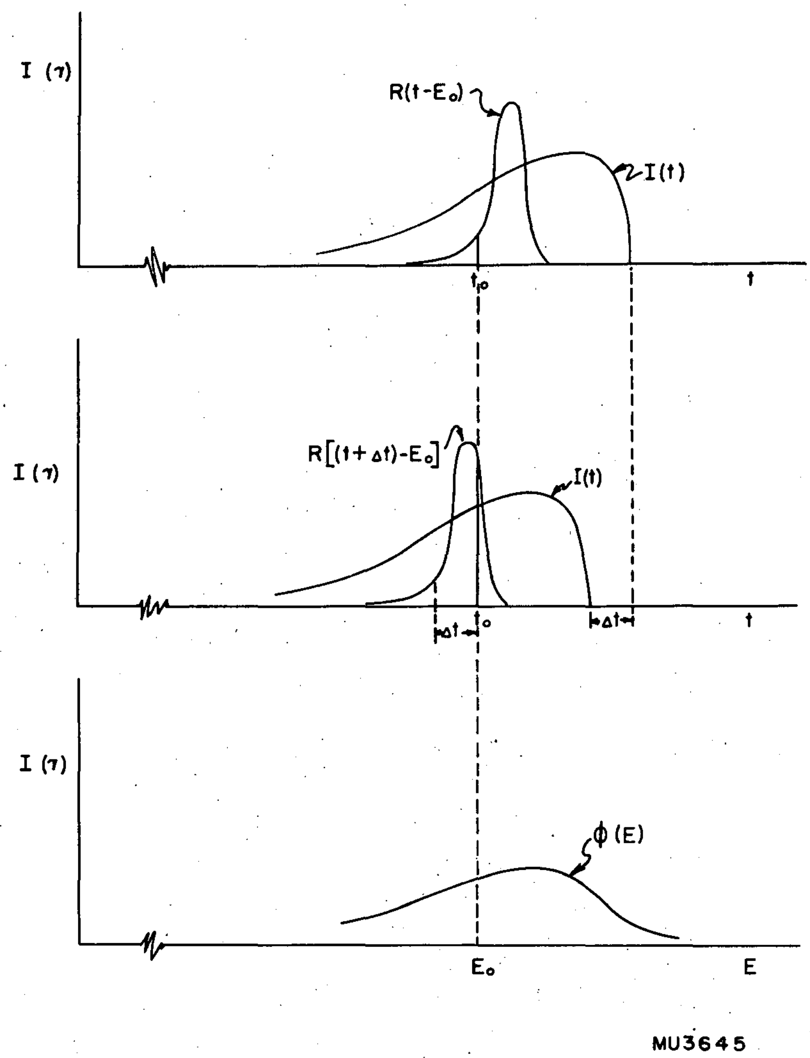

Fig. 4

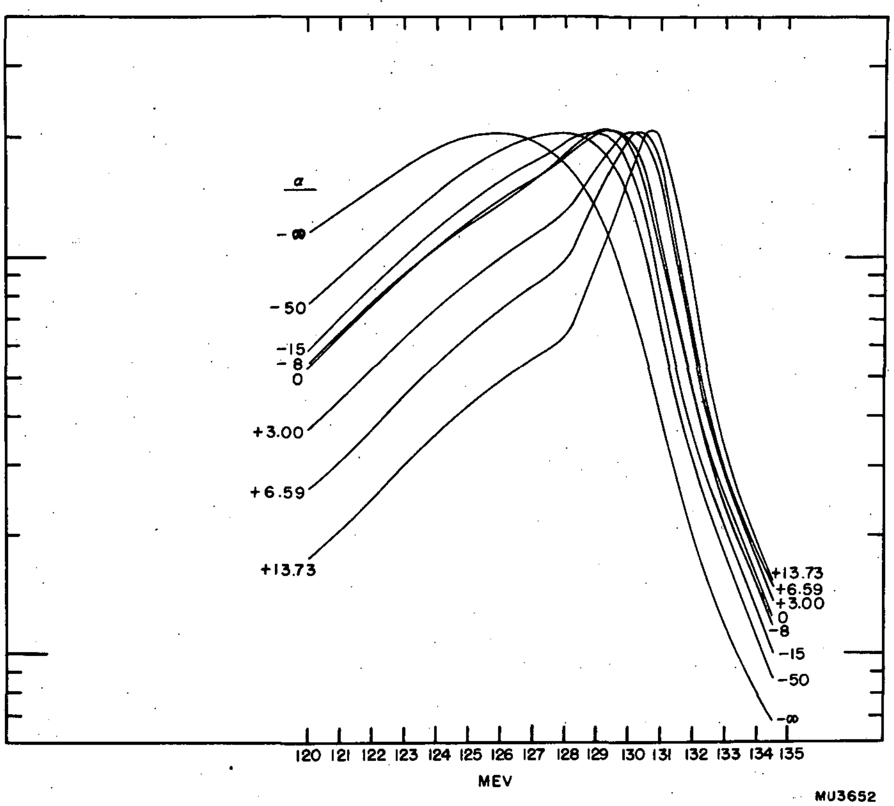

α
-∞
-50
-15
-8
0
+3.00
+6.59
+13.73
+13.73
+6.59
+3.00
0
-8
-15
-50
-∞
120 121 122 123 124 125 126 127 128 129 130 131 132 133 134 135
MEV
MU3652

Fig. 5

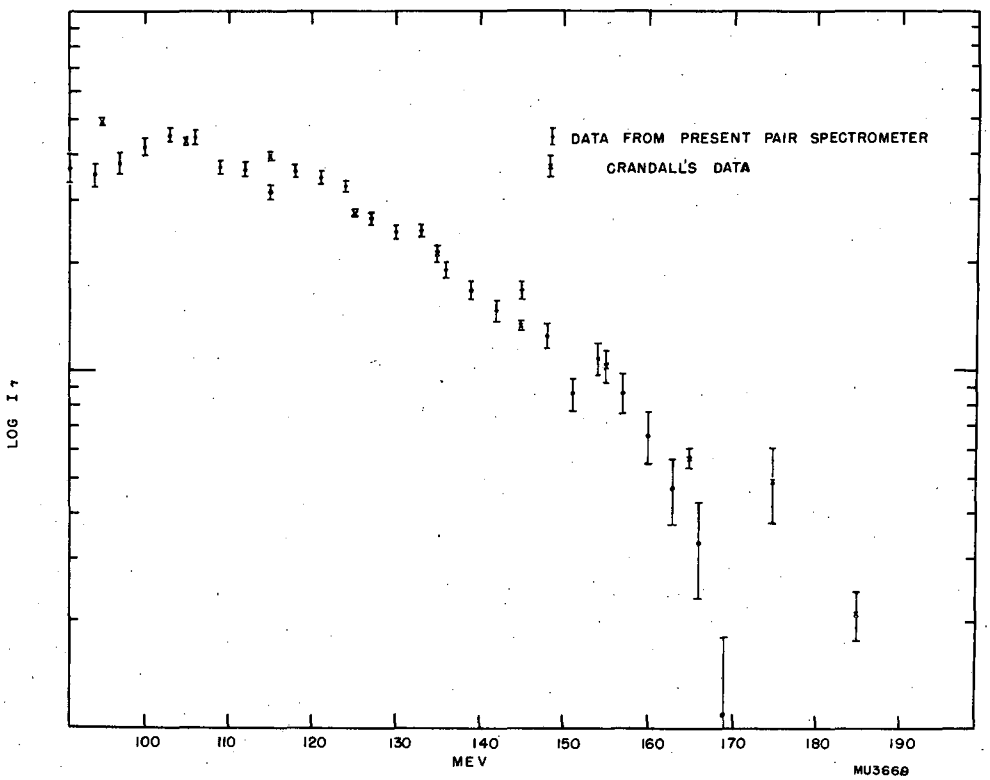
DATA FROM PRESENT PAIR SPECTROMETER
CRANDALL'S DATA
LOG I
100
110
120
130
140
150
160
170
180
190
MEV
MU3669

Fig. 6

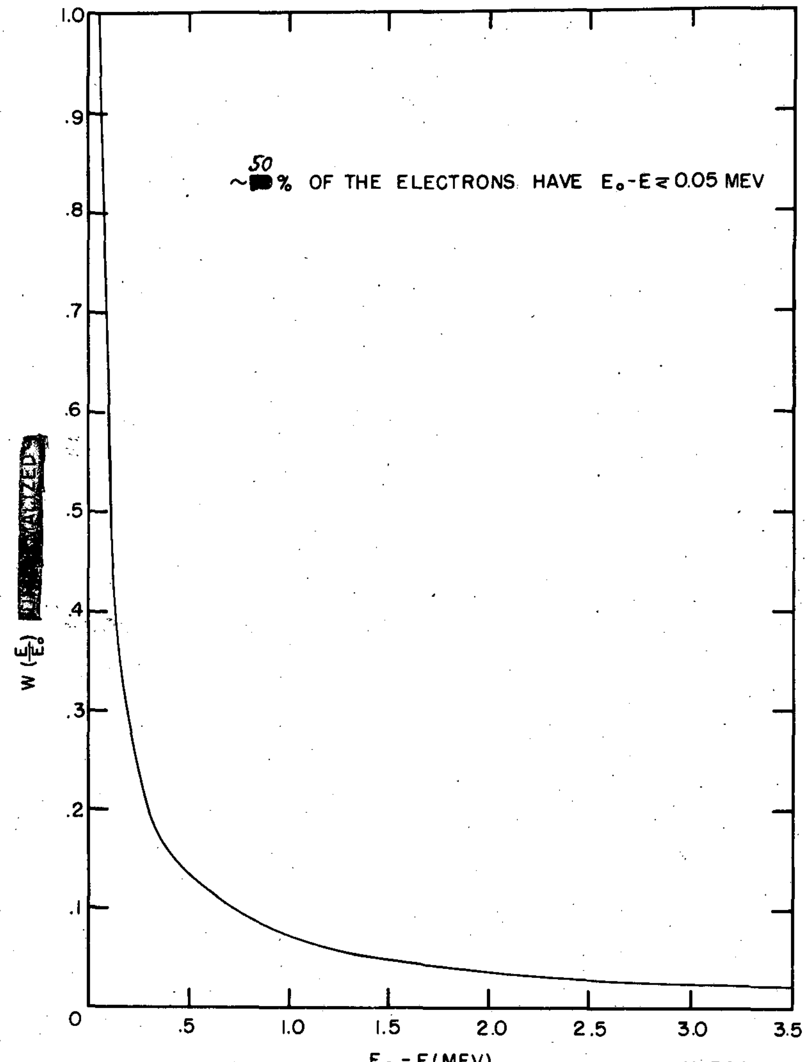
50
~[redacted]% OF THE ELECTRONS HAVE $E_0 - E \lesssim 0.05$ MEV
1.0
.9
.8
.7
.6
.5
.4
.3
.2
.1
0
.5
1.0
1.5
2.0
2.5
3.0
3.5
$W\left(\frac{E}{E_0}\right)$
$E_0 - E$ (MEV)

FIG. 7

MU3692

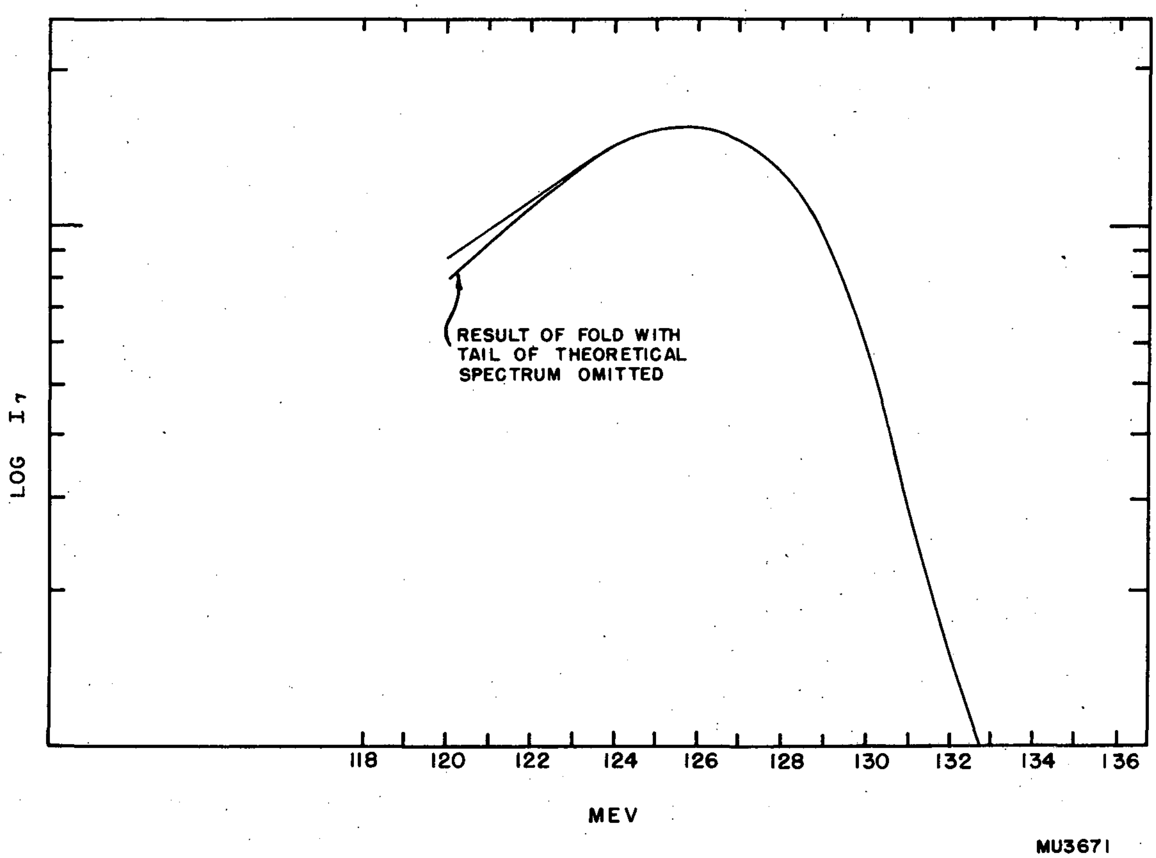

RESULT OF FOLD WITH
TAIL OF THEORETICAL
SPECTRUM OMITTED
LOG I$_\gamma$
118
120
122
124
126
128
130
132
134
136
MEV
MU3671

Fig. 8

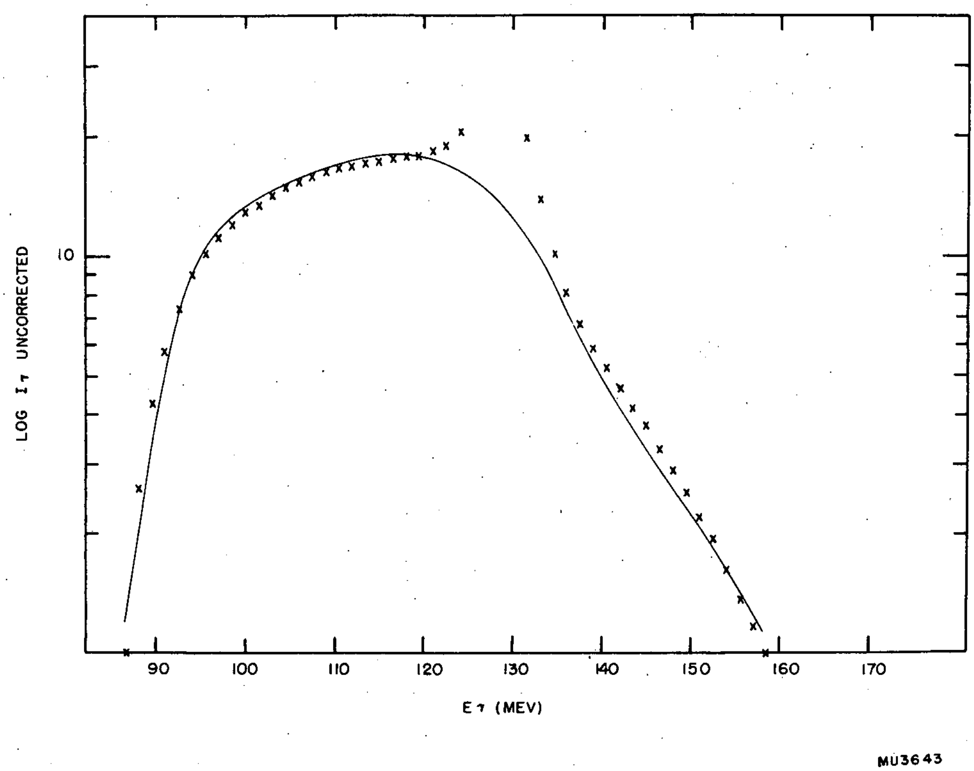

10
LOG I_γ UNCORRECTED
90
100
110
120
130
140
150
160
170
E_γ (MEV)
MU3643

Fig. 9

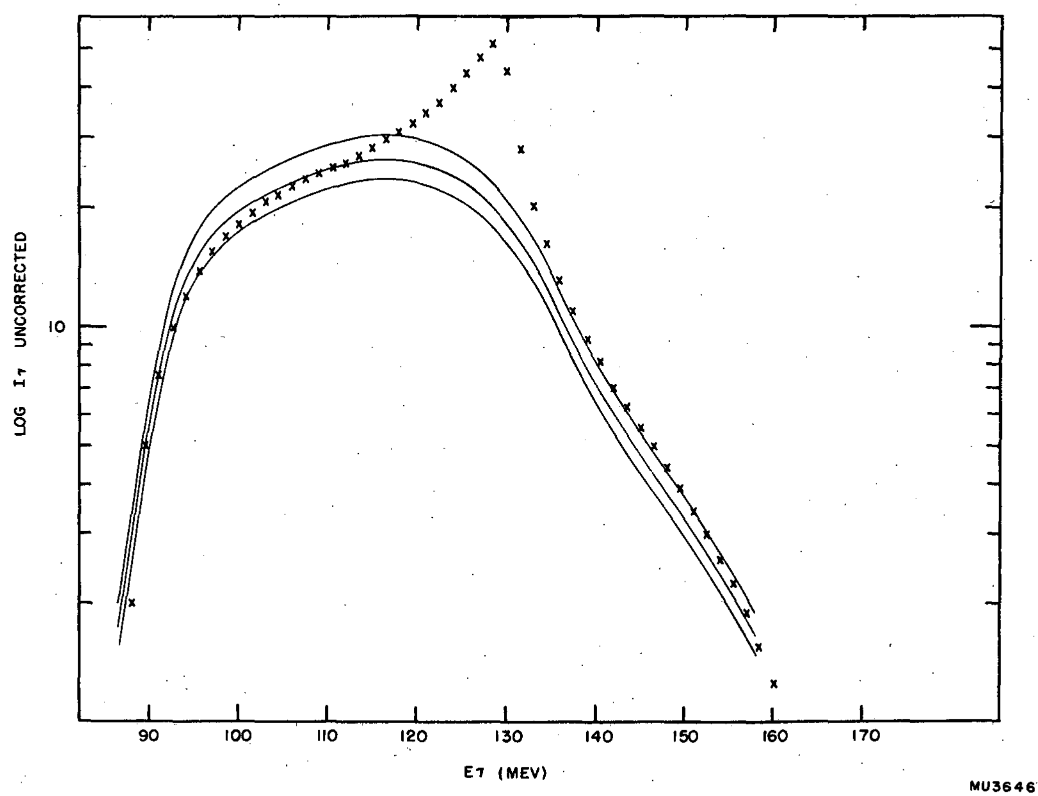

LOG I_γ UNCORRECTED
10
90
100
110
120
130
140
150
160
170
E_γ (MEV)
MU3646

Fig. 10

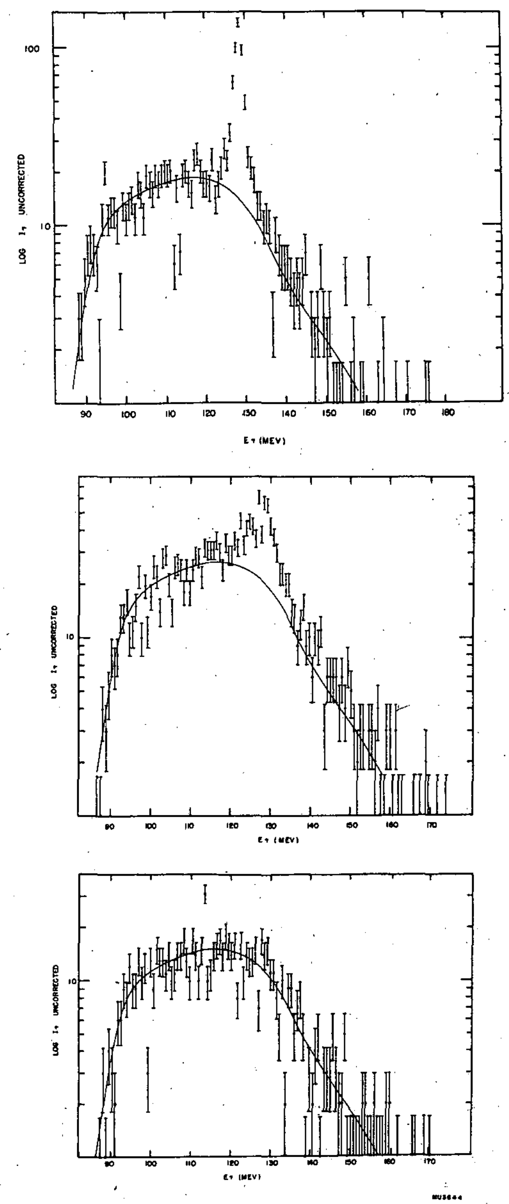

LOG I+ UNCORRECTED
100
10
90
100
110
120
130
140
150
160
170
180
E+ (MEV)
MU3644

Fig. 11

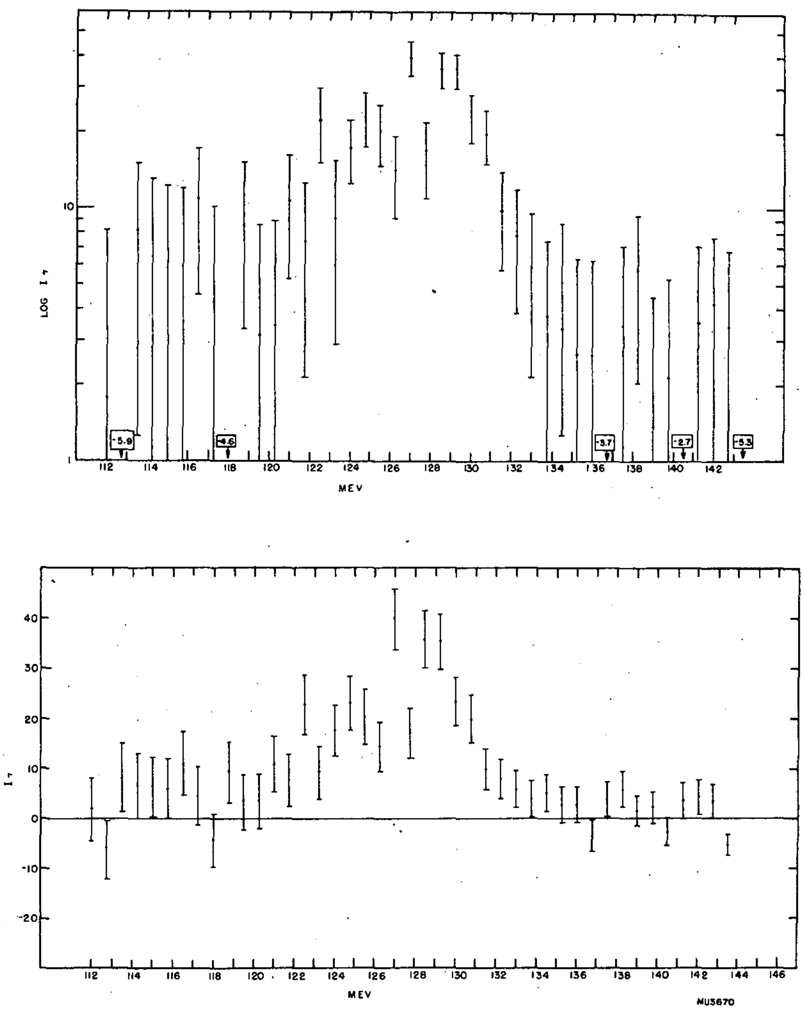
LOG I
10
1
-5.9
-4.6
-3.7
-2.7
-5.3
112
114
116
118
120
122
124
126
128
130
132
134
136
138
140
142
MEV
I
40
30
20
10
0
-10
-20
144
146
MU3670

Fig. 12

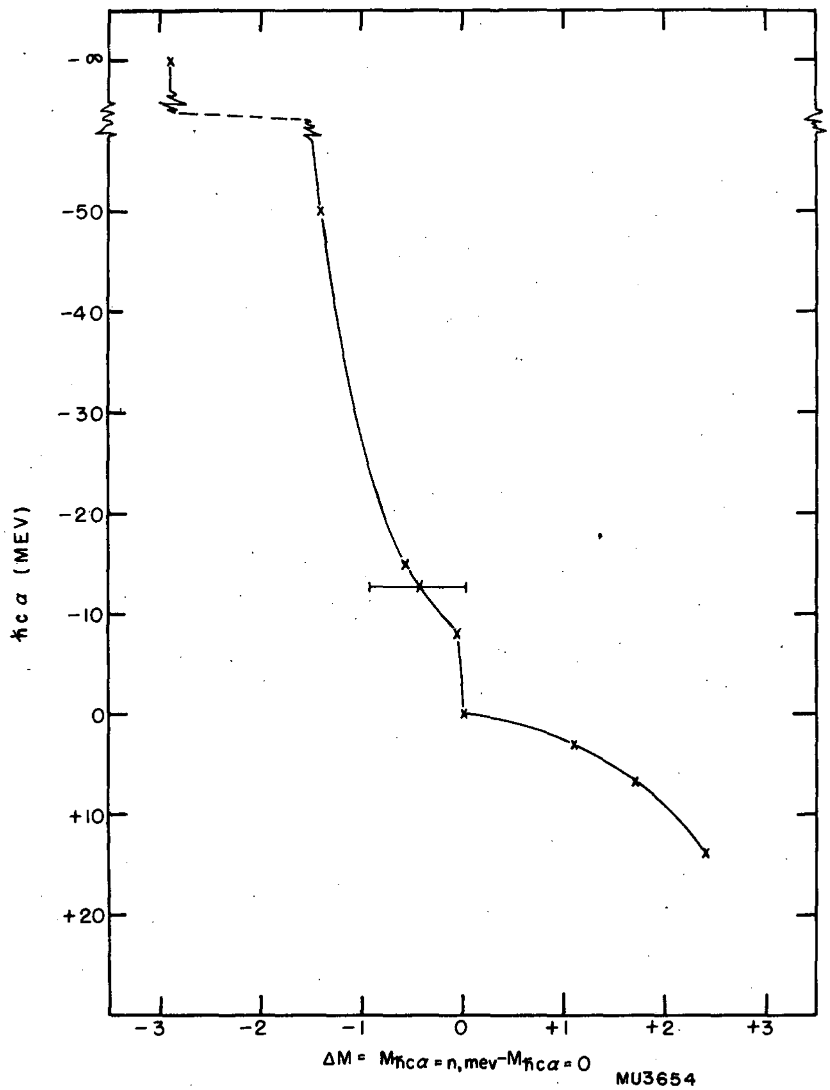

Fig. 13

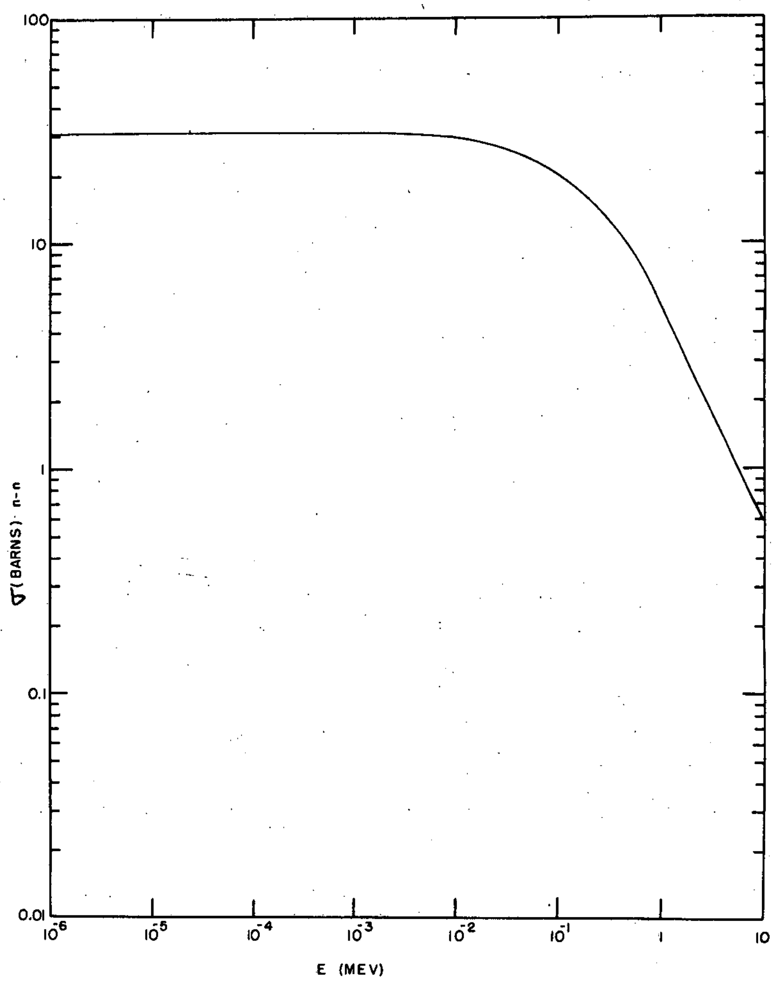

FIG. 14

MU3693